Cavity-enhanced laser absorption spectroscopy using microresonator whispering-gallery modes

G. Farca[1], S. I. Shopova[2], and A. T. Rosenberger[3*]

[1]Vescent Photonics Inc., 4865 E. 41st Ave., Denver, CO 80216, USA
[2]Biological Engineering Department, University of Missouri – Columbia, 240D Bond Life Sciences Center, 1201 E. Rollins Street, Columbia, MO 65211, USA
[3]Department of Physics, Oklahoma State University, Stillwater, OK 74078, USA
**Corresponding author: atr@okstate.edu*

Abstract: Tunable diode laser absorption spectroscopy using microresonator whispering-gallery modes (WGMs) is demonstrated. WGMs are excited around the circumference of a cylindrical cavity 125 μm in diameter using an adiabatically tapered fiber. The microresonator is very conveniently tuned by stretching, enabling the locking of an individual WGM to the laser. As the laser is scanned in frequency over an atmospheric trace-gas absorption line, changes in the fiber throughput are recorded. The experimental results of cavity-enhanced detection using such a microresonator are centimeter effective absorption pathlengths in a volume of only a few hundred microns cubed. The measured effective absorption pathlengths are in good agreement with theory.

OCIS codes: (350.3950) Micro-optics; (300.1030) Absorption; (230.5750) Resonators; (060.2370) Fiber optics sensors.

References and links

1. M. Cai, G. Hunziker, and K. Vahala, "Fiber-Optic Add-Drop Device Based on a Silica Microsphere-Whispering Gallery Mode System," IEEE Photon. Technol. Lett. **11**, 686-687 (1999).
2. S. I. Shopova, G. Farca, A. T. Rosenberger, W. M. S. Wickramanayake, and N. A. Kotov, "Microsphere whispering-gallery-mode laser using HgTe quantum dots," Appl. Phys. Lett. **85**, 6101-6103 (2004).
3. I. Teraoka, S. Arnold, and F. Vollmer, "Perturbation approach to resonance shifts of whispering-gallery modes in a dielectric microsphere as a probe of a surrounding medium," J. Opt. Soc. Am. B **20**, 1937-1946 (2003).
4. N. M. Hanumegowda, C. J. Stica, B. C. Patel, I. White and X. Fan, "Refractometric sensors based on microsphere resonators," Appl. Phys. Lett. **87**, 201107 (2005).
5. A. M. Armani and K. J. Vahala, "Heavy water detection using ultra-high-*Q* microcavities," Opt. Lett. **31**, 1896-1898 (2006).
6. A. T. Rosenberger and J. P. Rezac, "Whispering-gallery-mode evanescent-wave microsensor for trace-gas detection," Proc. SPIE **4265**, 102-112 (2001).
7. R. W. Boyd and J. E. Heebner, "Sensitive disk resonator photonic biosensor," Appl. Opt. **40**, 5742-5747 (2001).
8. M. L. Gorodetsky and V. S. Ilchenko, "Optical microsphere resonators: optimal coupling to high-*Q* whispering-gallery modes," J. Opt. Soc. Am. B **16**, 147-154 (1999).
9. M. Cai, O. Painter, and K. J. Vahala, "Observation of Critical Coupling in a Fiber Taper to a Silica-Microsphere Whispering-Gallery Mode System," Phys. Rev. Lett. **85**, 74-77 (2000).
10. A. T. Rosenberger, "Analysis of whispering-gallery microcavity-enhanced chemical absorption sensors," Opt. Express **15**, 12959-12964 (2007), http://www.opticsinfobase.org/abstract.cfm?URI=oe-15-20-12959.
11. M. J. Humphrey, E. Dale, A. T. Rosenberger, and D. K. Bandy, "Calculation of optimal fiber radius and whispering-gallery mode spectra for a fiber-coupled microsphere," Opt. Commun. **271**, 124-131 (2007).
12. J. P. Rezac and A. T. Rosenberger, "Locking a microsphere whispering-gallery mode to a laser", Opt. Express **8**, 605-610 (2001), http://www.opticsinfobase.org/abstract.cfm?URI=oe-8-11-605.
13. S.-I Chou, D. S. Baer, and R. K. Hanson, "Diode laser absorption measurements of CH_3Cl and CH_4 near 1.65 μm," Appl. Opt. **36**, 3288-3293 (1997).

#88097 - $15.00 USD Received 1 Oct 2007; revised 19 Oct 2007; accepted 21 Oct 2007; published 10 Dec 2007

14. A. Boschetti, D. Bassi, E. Iacob, S. Iannotta, L. Ricci, and M. Scotoni, "Resonant photoacoustic simultaneous detection of methane and ethylene by means of a 1.63-μm diode laser," Appl. Phys. B **74**, 273-278 (2002).
15. L. S. Rothman, C. P. Rinsland, A. Goldman, S. T. Massie, D. P. Edwards, J.-M. Flaud, A. Perrin, C. Camy-Peyret, V. Dana, J.-Y. Mandin, J. Schroeder, A. McCann, R. R. Gamache, R. B. Wattson, K. Yoshino, K. V. Chance, K. W. Jucks, L. R. Brown, V. Nemtchinov, and P. Varanasi, "The HITRAN Molecular Spectroscopic Database and HAWKS (HITRAN Atmospheric Workstation): 1996 Edition," J. Quant. Spectrosc. Radiat. Transfer **60**, 665-710 (1998).
16. W. von Klitzing, R. Long, V. S. Ilchenko, J. Hare, and V. Lefèvre-Seguin, "Tunable whispering gallery modes for spectroscopy and CQED experiments," New J. Phys. **3**, 14.1-14.14 (2001), http://www.iop.org/EJ/article/1367-2630/3/1/314/nj1114.pdf?request-id=OB3CCdlt3BGvpWIl3Ai7Kg.

1. Introduction

Whispering-gallery modes (WGMs) in dielectric microresonators have been studied extensively over the past several years because of their high quality factors (Q) and low mode volumes, characteristics suitable for a wide range of applications including optical add-drop devices [1], microlasers [2], and chemical sensors [3-7]. So far, in label-free chemical sensing applications, the interaction of a WGM's evanescent component with an analyte in the ambient or adsorbed on the microresonator's surface has led to the development of two sensing methods. These are: monitoring of the WGM resonance frequency shift due to the analyte's change of the effective index of refraction [3,4], and measurement of the amount of Q spoiling resulting from analyte absorption [5].

Another method that we introduced earlier [6] and further develop here is based on recording changes in the resonant dip depth observed in the coupling-fiber throughput [7]. We use a cylindrical microcavity for which a WGM is excited around the circumference using an adiabatically tapered fiber tangentially in contact with the microcavity. Tunable diode laser light is injected at one end of the tapered fiber and the throughput at the other end will display a Lorentzian dip every time a WGM resonance is excited. The analysis of such an efficiently coupled microcavity is well known [7-9]. Absorption by a molecular trace gas in the air surrounding the microresonator will change the depth of a resonant dip, and this change is what we measure. This method enables tunable diode laser absorption spectroscopy experiments in which the long effective absorption pathlengths that result are confined within less than a cubic millimeter.

Although the cylindrical microresonators provide a lower sensitivity than the microspheroids used earlier [6] (however, see further discussion in Section 5), they offer some very attractive advantages. First, they are far easier to mount in a strain tuner, and are much less susceptible to mechanical failure than microspheroids tuned by compression. Second, alignment is easier since there is only one degree of freedom to adjust (making the taper perpendicular to the cylinder axis), versus two for the spheroids. Third, the mode spectrum is sparser, making locking easier. And, finally, because the microcylinder is just a standard optical fiber, different resonators are nearly identical in diameter, providing better repeatability of results.

2. Theory of operation

For chemical sensing applications, we model the microresonator as a ring cavity with internal loss in which one of the mirrors is partially transmitting while all the others are assumed to be perfectly reflective [10]. This model is a valid analog to a fiber-coupled microresonator when only a single fiber mode is excited; this is accomplished by making the fiber taper transitions adiabatic, and by properly choosing the diameter of the tapered fiber [10,11].

The depth of a resonant dip in the fiber throughput is dependent on the ratio x of the coupling loss to the intrinsic loss of the microresonator and is given by:

$$M_0 = \frac{4x}{(1+x)^2}. \tag{1}$$

#88097 - $15.00 USD Received 1 Oct 2007; revised 19 Oct 2007; accepted 21 Oct 2007; published 10 Dec 2007

The microresonator is said to be undercoupled if the value of x is less than unity and overcoupled if the value of x is greater than unity.

While the coupling loss of the microresonator remains constant, the effective intrinsic loss is modified by analyte absorption in the evanescent fraction f of the WGM. The effective loss coefficient can then be written as $\alpha = \alpha_i + f\alpha_a$, where α_i is the actual intrinsic loss coefficient and α_a is the analyte absorption coefficient. Absorption by the analyte causes a small change in dip depth that is proportional to the analyte absorption coefficient [10]. When a WGM is frequency-locked [12] to the input laser, the WGM stays on resonance with the laser and, as the laser scans in frequency, the throughput of the bi-tapered fiber displays the locus of the bottom of the WGM resonance dip as it follows the laser scan. When an absorption line of the surrounding gas is present within the scan there is a change in the WGM dip depth that traces the contour of the respective absorption line. Since in such a setup the microresonator is always on resonance, light interacting with the gas executes many round trips around the circumference, resulting in a long effective interaction path length.

Theoretically, an effective absorption path length can be obtained from the dip depth dependence on the absorption coefficient of the analyte, making the analogy with Beer's law:

$$\frac{dM_0}{M_0} \cong -\left(\frac{1-x}{1+x}\right)\frac{f}{\alpha_i}\,d\alpha_a \cong -L_{eff}^{t}\,d\alpha_a\,. \tag{2}$$

Therefore, the theoretical effective absorption path length L_{eff}^{t} can be expressed as:

$$L_{eff}^{t} = \left(\frac{1-x}{1+x}\right)\frac{f}{\alpha_i}, \tag{3}$$

which holds in the low-analyte-absorption limit, $\alpha_a L_{eff}^{t} << 1$ (or $f\alpha_a << \alpha_i$). Likewise, the experimental effective absorption path length L_{eff}^{e} takes the form

$$L_{eff}^{e} = \frac{1}{\alpha_a}\ln\frac{M_0}{M_0 + \Delta M_0}, \tag{4}$$

and is found by measuring the dip depth in the absence of analyte (M_0) and in the presence of analyte ($M_0 + \Delta M_0$). Equation (4) thus provides a way to express the relative sensitivity (fractional change in dip depth) of the WGM gas sensor based on the experimental effective absorption pathlength, the length of a hypothetical absorption cell that has the same sensitivity. The model is tested by comparing experimental and theoretical effective pathlengths.

3. Experimental setup

Figure 1 shows the experimental setup. A cylindrical vacuum chamber with a transparent top plate and side windows for viewing the optical setup is connected to a reference cell that is used for calibration. The gas mixes and pressures in the chamber and cell can be varied independently. Typically, a low partial pressure of the molecular gas of interest is added to air at atmospheric pressure in the main chamber. Light from a cw tunable diode laser (TDL) is coupled into the reference cell and into a single-mode optical fiber. The fiber passes through a polarization controller that is adjusted to ensure that WGMs of a single polarization (TE or TM) are excited. Then the fiber is fed into the vacuum chamber where its adiabatic bi-taper is brought into contact with the microresonator. The position and orientation of the coupling fiber are controlled, via bellows-sealed feedthroughs, by a positioner located outside the chamber. The 125-μm-diameter cylindrical fused-silica microresonator is mounted in a fixture (inset, Fig. 1) that allows tuning of the WGMs by stretching the resonator when a voltage is applied to the piezoelectric transducer (PZT). The microcylinder is just a standard

#88097 - $15.00 USD Received 1 Oct 2007; revised 19 Oct 2007; accepted 21 Oct 2007; published 10 Dec 2007

optical fiber whose jacket has been softened by soaking in acetone and then pulled off. The fiber is then soaked in clean acetone and wiped with lens paper and methanol. This preserves the optical quality of the microresonator's surface. After the coupling fiber exits the chamber its output is collected onto a detector. The signal from the detector is split, part of it being fed into a lock-in stabilizer in order to lock individual WGMs to the laser.

The locking is done as follows [12]. A WGM is tuned to be in resonance with the TDL by adjusting the PZT bias voltage, and the lock-in stabilizer is switched on. The lock-in stabilizer applies a 518-Hz dither voltage to the PZT and peak-locks the WGM to the laser. Then as the laser scans in frequency the lock-in stabilizer tunes the dc bias voltage on the PZT, maintaining the WGM on resonance with the laser over the entire scan range. When locked, the maximum excursion from true resonance is less than 5% of the WGM's linewidth. This tuning jitter results in unfiltered noise on the signal that is less than 1% of the dip depth.

The rest of the detector signal is noise filtered and amplified by a lock-in amplifier. The output of the lock-in amplifier is monitored by an oscilloscope, and recorded as the laser scans across the gas's absorption line. The result is a spectral profile of the gas absorption, impressed on the depth of the locked resonance dip. This is then analyzed using Eq. (4) to find an experimental effective absorption path length.

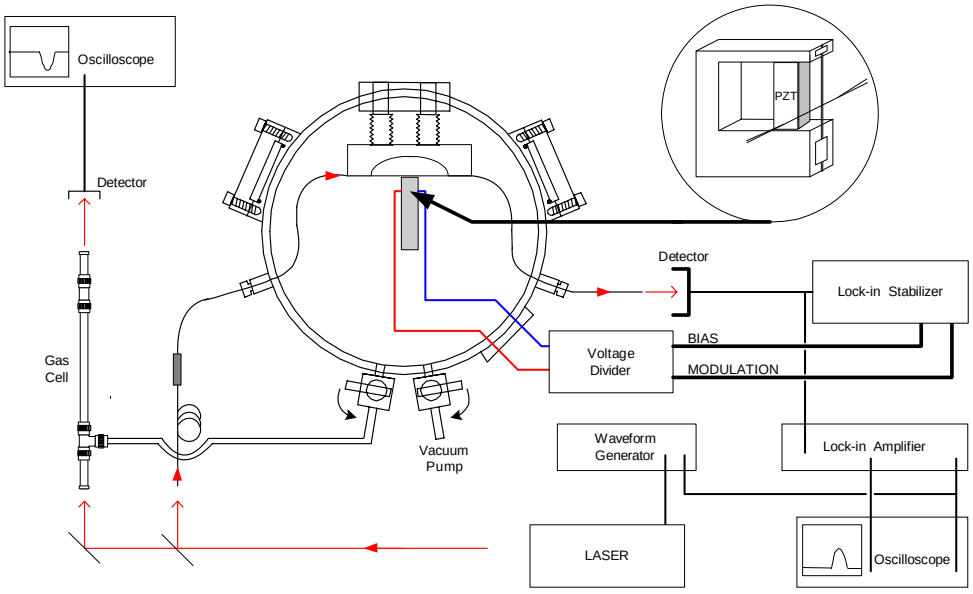

Fig. 1. Experimental setup. Light from a frequency-scanned cw diode laser (red) is launched into a bi-tapered fiber to excite WGMs of the microresonator. The microresonator is held in a PZT fixture for tuning purposes (inset.)

4. Results

Experimental results are reported here for a few trace gases, having absorption features in the vicinity of 1.65 μm, in air at atmospheric pressure. The gases investigated were methane (CH_4) [13,14], methyl chloride (CH_3Cl) [13], and ethylene (C_2H_4) [14]. The transitions involved belong to overtone and combination bands involving the C-H bonds. For example, the absorption lines of methane in this wavelength range correspond to the C-H asymmetric stretch vibrational overtone $2v_3$ [13-15]. There are three lines of approximately equal strength that are roughly equally spaced at intervals of about 400 MHz and pressure broadened by air

#88097 - $15.00 USD Received 1 Oct 2007; revised 19 Oct 2007; accepted 21 Oct 2007; published 10 Dec 2007

to about 4 GHz each [15]. The methyl chloride lines probably belong to the perpendicular component of the $2\nu_4$ band [13]; however, the assignment for ethylene is less certain [14].

These results are presented in Fig. 2 and the details are summarized in Table 1. For each gas in Fig. 2, the dip depth variation (change in M_0, at 50× amplification) shows the detected absorption profile. These are not to scale, in the sense that the full dip is far too large to show at this amplification. Straight lines are added to make the variation clear; the slope of these lines (again, amplified 50×) may be an effect of the differential tuning of adjacent WGMs, because there is no variation in coupling (or in x) over the 10-GHz frequency scan range. When the gas compositions and pressures are the same in the test chamber and in the reference cell, both give the same lineshape. For example, the top traces in Fig. 2 (methane) can be fit well by a sum of three unresolved Lorentzians.

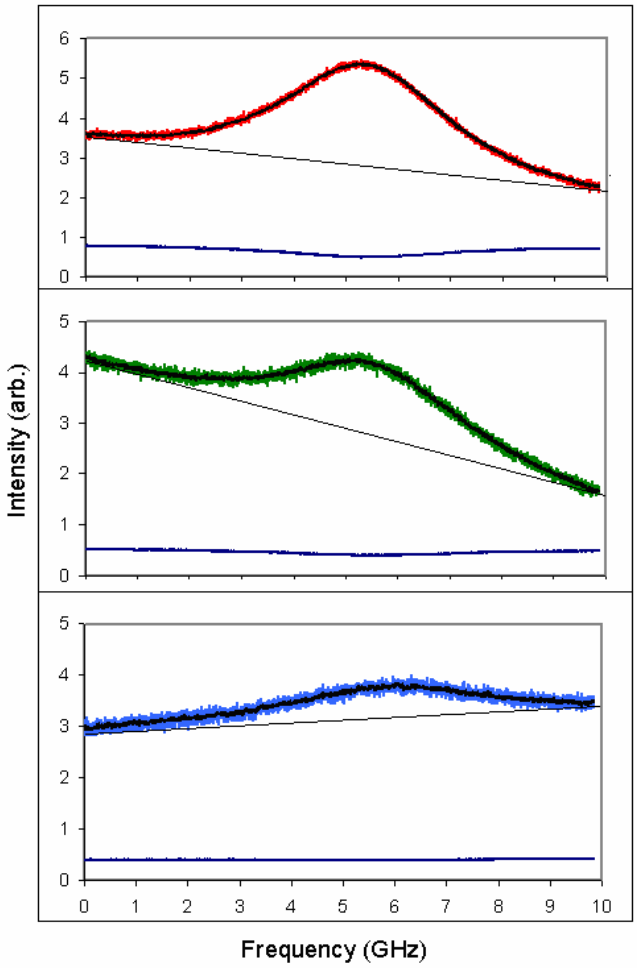

Fig. 2. From top down: the measured absorption profiles of methane, methyl chloride, and ethylene obtained using a WGM locked to the laser. In each case, the top trace shows the amplified variation in dip depth and the bottom trace is the transmission profile of the gas in a 16-cm absorption cell. The frequency axis shows the tuning range.

In Table 1, the theoretical effective absorption pathlength is calculated from Eq. (3) using, for example, in the case of methane, $x = 0.28$ (calculated from the dip depth M_0; the dip gets shallower with analyte absorption, so the WGM is undercoupled), $f = 1.6\%$ (estimated from a computation of the field distributions at the same wavelength in a microsphere of the

#88097 - $15.00 USD Received 1 Oct 2007; revised 19 Oct 2007; accepted 21 Oct 2007; published 10 Dec 2007

same diameter), and α_i = 0.0061 cm^{-1} (found from the values of Q and x). The experimental effective absorption pathlength was obtained using Eq. (4) in which, again for methane, M_0 = 68.4% and ΔM_0 = -0.7%. The value of the methane absorption coefficient that was used for this concentration, α_a = 0.0058 cm^{-1}, was extracted from the reference cell transmission measurements, and is in reasonable agreement with the value expected from parameters found in the HITRAN database [15]. Similar calculations were done for the other gases.

Table 1. Summary of results from Fig. 2, for gases in air at atmospheric pressure.

Gas	L^t_{eff} **(mm)**	L^e_{eff} **(mm)**	**WGM** Q	λ **(nm)**	**Partial pressure**
CH_4	15.0± 3.0	17.7 ± 1.7	7×10^6	1653.722	0.01 atm
CH_3Cl	7.2 ± 1.5	6.3 ± 1.1	3×10^6	1651.59	0.01 atm
C_2H_4	13.6 ± 2.7	13.2 ± 2.6	5×10^6	1654.23	0.02 atm

For each trace gas in Table 1 there is good agreement between the theoretical and experimental effective absorption path lengths. For the theoretical values the main source of error is in calculating the evanescent fraction, because it takes on different values for different modes, and the WGM that is used is not definitively identified. Uncertainty in the measured value of α_a and the residual noise on the traces corresponding to the locked WGMs are responsible for the error in determining the experimental effective absorption path length.

5. Conclusions

Cavity-enhanced laser absorption spectroscopy using microresonator WGMs has been demonstrated by locking the WGM resonances to the laser. Atmospheric trace gases in the evanescent fraction of the locked WGM are detected. The gas molecules remain in the ambient air and are not adsorbed onto the microresonator surface. The relative detection sensitivity is characterized by an effective absorption pathlength, and its experimentally determined value is in good agreement with the theoretical prediction. The major advantages of our setup are miniaturization and relatively low cost. Although the detection volume is less than a cubic millimeter, relatively large effective absorption pathlengths on the order of centimeters are obtained.

From Fig. 2, the detection limit can be estimated to be about one-tenth of the concentrations shown, or about 1000 parts per million. This is an order of magnitude higher than that estimated for a microsphere in Ref. [6], because the Q is lower by a factor of twenty -- 5×10^6 versus 10^8. The other advantages of the microcylinder mentioned in the Introduction outweigh this sensitivity deficit and, in addition, we now have very good agreement with theory. Nevertheless, other microresonator geometries can also be envisioned for enhancing the sensitivity of the setup. Using a fiber fusion splicer, for example, a microspheroidal resonator with two stems can be obtained. Mounting it into the same PZT device would enable tuning of the WGMs in the same fashion as the microcylinder [16]. However, the curved surfaces of the microspheroid should, in principle, result in higher-Q WGMs with greater detection sensitivities, i.e., longer effective absorption pathlengths.

Acknowledgments

This work was supported by the Oklahoma Center for the Advancement of Science and Technology under project number AR022-052 and by the National Science Foundation under award number ECS-0329924. The authors thank J. P. Rezac, D. K. Bandy, and M. J. Humphrey for assistance, and M. Lucas for instrument construction.

#88097 - $15.00 USD Received 1 Oct 2007; revised 19 Oct 2007; accepted 21 Oct 2007; published 10 Dec 2007